



Update on the Comparison of Second-Order Loads on a Tension Leg Platform for Wind Turbines

Preprint

Sébastien Gueydon

Maritime Research Institute of the Netherlands

Jason Jonkman

National Renewable Energy Laboratory

*Presented at the Twenty-sixth (2016) International Ocean and
Polar Engineering Conference (ISOPE)*

Rhodes, Greece

June 26–July 2, 2016

**NREL is a national laboratory of the U.S. Department of Energy
Office of Energy Efficiency & Renewable Energy
Operated by the Alliance for Sustainable Energy, LLC**

This report is available at no cost from the National Renewable Energy
Laboratory (NREL) at www.nrel.gov/publications.

Conference Paper

NREL/CP-5000-65993

August 2016

Contract No. DE-AC36-08GO28308

NOTICE

The submitted manuscript has been offered by an employee of the Alliance for Sustainable Energy, LLC (Alliance), a contractor of the US Government under Contract No. DE-AC36-08GO28308. Accordingly, the US Government and Alliance retain a nonexclusive royalty-free license to publish or reproduce the published form of this contribution, or allow others to do so, for US Government purposes.

This report was prepared as an account of work sponsored by an agency of the United States government. Neither the United States government nor any agency thereof, nor any of their employees, makes any warranty, express or implied, or assumes any legal liability or responsibility for the accuracy, completeness, or usefulness of any information, apparatus, product, or process disclosed, or represents that its use would not infringe privately owned rights. Reference herein to any specific commercial product, process, or service by trade name, trademark, manufacturer, or otherwise does not necessarily constitute or imply its endorsement, recommendation, or favoring by the United States government or any agency thereof. The views and opinions of authors expressed herein do not necessarily state or reflect those of the United States government or any agency thereof.

This report is available at no cost from the National Renewable Energy Laboratory (NREL) at www.nrel.gov/publications.

Available electronically at SciTech Connect <http://www.osti.gov/scitech>

Available for a processing fee to U.S. Department of Energy and its contractors, in paper, from:

U.S. Department of Energy
Office of Scientific and Technical Information
P.O. Box 62
Oak Ridge, TN 37831-0062
OSTI <http://www.osti.gov>
Phone: 865.576.8401
Fax: 865.576.5728
Email: reports@osti.gov

Available for sale to the public, in paper, from:

U.S. Department of Commerce
National Technical Information Service
5301 Shawnee Road
Alexandria, VA 22312
NTIS <http://www.ntis.gov>
Phone: 800.553.6847 or 703.605.6000
Fax: 703.605.6900
Email: orders@ntis.gov

Cover Photos by Dennis Schroeder: (left to right) NREL 26173, NREL 18302, NREL 19758, NREL 29642, NREL 19795.

NREL prints on paper that contains recycled content.

Update on the Comparison of Second-Order Loads on a Tension Leg Platform for Wind Turbines

Sébastien Gueydon¹, Jason Jonkman²

¹Maritime Research Institute of The Netherlands (MARIN)
Wageningen, The Netherlands

²National Renewable Energy Laboratory (NREL)
Golden, Colorado, USA

ABSTRACT

In comparison to other types of floaters (like a spar or a semisubmersible), the Tension Leg Platform (TLP) has several notable advantages: its vertical motions are negligible, its weight is lighter, and its mooring system's footprint is smaller. While a TLP has a negligible response to first-order vertical wave loads, second-order wave loads need to be addressed. This paper follows up on a verification study of second-order wave loads on a TLP for wind turbines done by MARIN and NREL (Gueydon, Wuillaume, Jonkman, Robertson and Platt, 2015) and corrects some of its conclusions.

KEY WORDS: TLP; second-order hydrodynamics; structural flexibility; FAST; aNySIM; WAMIT; DIFFRAC.

INTRODUCTION

The design of floating offshore wind turbines requires sophisticated numerical tools capturing the coupled aerodynamics, hydrodynamics, control and electrical-drive dynamics, and structural dynamics of the full system nonlinearly in the time domain. The inherent sophistication of these tools warrants model-to-model verification, both at the module and integrated levels.

In previous works, we verified the hydrodynamic wave-body interaction with first- and second-order potential-flow solutions for a semisubmersible (Gueydon, Duarte and Jonkman, 2014) and a TLP (Gueydon, Wuillaume, Jonkman, Robertson and Platt, 2015) by comparing two tools—FAST (Jonkman and Buhl, 2005), which is developed by NREL, and aNySIM (Maritime Research Institute Netherlands, 2009), which is developed by MARIN. In these works, WAMIT (developed by WAMIT, Inc.) (Lee and Newman, 2013) and DIFFRAC (developed by MARIN) (Bunnik, 2012) were used to generate the first- and second-order potential-flow hydrodynamic radiation and diffraction solutions in the frequency domain using the boundary element method, which are transformed to the time domain within FAST and aNySIM, respectively.

In the study of the TLP, it appeared that the TLP, seen as a fully rigid body, had little sensitivity to second-order loads whereas this sensitivity was large when the tower flexibility was accounted for. The effect of

the flexibility of the tower was studied with a prototype version of FAST v8 (FAST Dev), which included an early implementation of the second-order wave loads before the first official release (FAST v8.10). The comparison of the motions of the TLP with the flexible tower against those of the fully rigid TLP showed a significant increase of the pitch response. It was concluded that this increase was a direct consequence of the shift of the pitch eigenfrequency for the TLP with the flexible tower to a lower value where the sum-frequency loads were almost at their maximum. It was observed with the prototype program that second-order high-frequency wave loads were big enough to trigger a resonance response of the pitch/tower first bending mode of the TLP. Nevertheless, these results could not be reproduced in the official release of FAST v8.10. Therefore, MARIN and NREL investigated possible causes of this major difference. It was found that an error in the prototype caused an exaggeration of second-order wave loads, which were then large enough to result in a noticeable amplification of the pitch motion previously reported. This problem, which reflects the “teething pains” inherent in any major upgrade of a program, was identified and solved before the release of FAST v8.10. The present paper gives the correct results of the simulations of the TLP with the flexible tower and updated conclusions.

TLP MODEL

TLP Description

In 2011, the DeepCwind consortium came to MARIN to test three different types of floating support platforms for a horizontal-axis wind turbine: a spar, a TLP and a semi-submersible. All three floaters, with the same turbine on top, were tested in the Offshore Basin of MARIN under both wind and wave excitation. The present work looks at the behavior of the TLP in waves using numerical simulations. The TLP is only placed in long crested head waves. There is no wind, and the turbine is parked. The TLP is moored in 200-m water depth by three tendons with an equal pretension of 4837 kN. The mooring system is modeled as a spring. Table 1 gives the most relevant characteristic data for the work presented in this paper. However, more details can be found in other technical publications (Goupee, Koo, Lambrakos and Kimball, 2012; Prowell, Robertson, Jonkman, Stewart and Goupee, 2013). Note that the floater characteristics, its response and the wave loads are all represented at full scale in this paper whereas the actual model tests were done at 1/50th scale based on Froude scaling.

Table 1. Characteristics of the moored TLP with the turbine on top as built for the model tests of 2011.

	Symbol	Units	Values
Mass	M	kg	1361E3
Displacement	Δ	m ³	2770.7
Draft	T	m	30.0
Centre of gravity above keel	KG	m	64.06
Pitch radius of inertia (about KG)	k_{yy}	m	52.69
Angle between each pontoon		deg	120
Tendon pre-tension	T_p	N	4837E3
Tendon axial stiffness	EA	N	8.29E9

Comparison Study for the Rigid TLP

A potential-flow model of the TLP was made. The same mesh of the immersed part of the TLP was used for both potential-flow numerical tools (Fig. 1):

- DIFFRAC of MARIN
- WAMIT of WAMIT Inc.

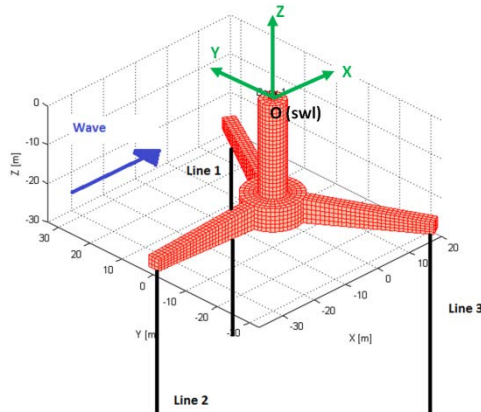


Fig. 1: Geometry of the TLP and conventions.

From this model, the geometry was used to determine the coefficients for the added mass, the potential damping and the linear wave-excitation loads. Several meshes with an increasing number of panels were used to ensure that the first-order solution had converged. All results in this paper are given at the point O of Fig. 1, which is located at the midship, center, still water level (swl). As the waves travel in the direction of the surge (x) axis of Fig. 1 and the rotor is not spinning, only quantities related to the surge and heave translations (z) and the pitch rotation (about y) are presented.

The comparison was done in two steps (Fig. 2). To start with, linear potential-flow calculations were carried out using DIFFRAC and WAMIT. The results of these calculations were compared (i.e., added mass, potential damping and wave load transfer functions). Using an equivalent stiffness matrix (Table 2) for the mooring system, simulations were run with aNySIM and FAST, and these simulation results were also compared.

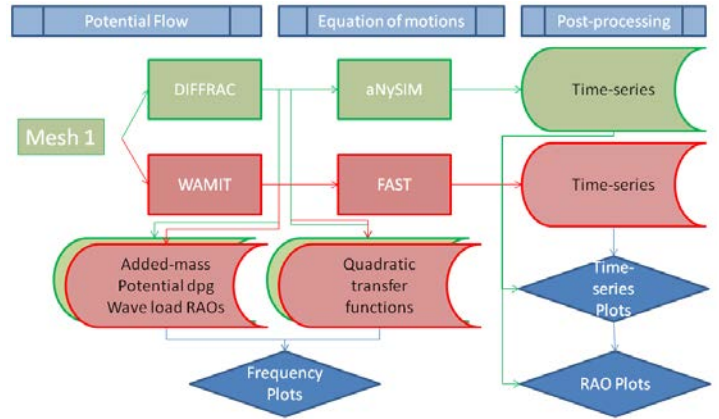


Fig. 2: Comparison of first order and second order results.

Once the first-order motion responses are known, the second-order can be calculated. The convergence of the second-order solution was also checked by using meshes with an increasing number of panels. Here again, two kinds of comparison are possible as explained. Firstly, it can be checked that the Quadratic Transfer Functions (QTF) resulting from DIFFRAC and WAMIT are similar. Secondly, simulations using these QTFs with aNySIM and FAST can be compared. This has been done and reported for the rigid TLP (Wuillaume, 2014).

Table 2. Spring characteristics.

	Symbol	Units	Values
Hydrostatic stiffness along z axis	C_{33}	N/m	3.33E5
Hydrostatic stiffness around y axis	$C_{55/O}$	N.m/rad	-6.31E8
Tendon stiffness along x axis	K_{11}	N/m	8.46E4
Tendon stiffness along z axis	K_{33}	N/m	1.45E8
Tendon stiffness around y axis	$K_{55/O}$	N.m/rad	6.54E10
Tendon stiffness x-z coupling	K_{13}	N/m	3.8E2

The eigenmodes of the TLP when modeled as a rigid body were determined from the system mass and hydrostatic/tendon stiffness terms and the linear solution of the potential-flow problem. Table 3 contains the frequencies of the main rigid-body modes. In addition to the radiation contribution of the potential-flow theory to the damping, viscous loads were added to the hydrodynamic loading. The viscous effects were introduced in the model by additional linear damping coefficients. The role of this additional damping is to limit the amplitude of the resonance peaks occurring at the frequencies of Table 3. Therefore, the additional damping is expressed as a percentage of the critical damping for each mode. The origin of this damping is discussed below. The same additional damping was used for both codes.

Table 3. Eigenfrequencies of the whole system seen as a rigid body.

Eigenmodes and viscous damping	Symbol	rad/s	Percent of critical damping
Translation along x axis (Surge)	ω_1	0.15	2.5
Translation along z axis (Heave)	ω_3	6.3	2.5
Rotation around y axis (Pitch)	ω_5	3.1	2.7

Knowing where resonance may happen, a suitable range of frequencies can be chosen for the second-order wave loading so that the calculation

of the QTF is limited to the most relevant frequency range. The amplitudes of the difference-frequency QTF in surge and the sum-frequency QTF in pitch are shown in Figs. 3 and 4, respectively. These QTFs are made dimensionless by applying the same expressions as in WAMIT's chapter 11 (Lee and Newman, 2013). The difference-frequency QTF is determined using first-order results for a frequency range of $[0.05; 1.6]$ rad/s where there is significant wave energy. The bandwidth of the QTF is chosen so that it largely contains the surge eigenfrequency (Fig. 3). The two black dotted lines plotted on Fig. 3 show the difference frequency equal to the surge eigenfrequency. The sum-frequency QTF is calculated based on first-order results from $[0.3; 3.5]$ rad/s so that the sum-frequencies include the pitch and the heave eigenfrequencies. The sum frequency equal to the pitch eigenfrequency of the rigid TLP is drawn in Fig. 4 with a black dotted line.

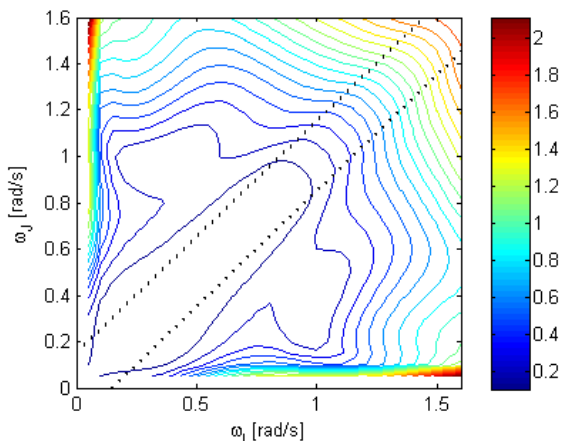


Fig. 3: Nondimensional amplitude of surge difference-frequency QTF of DIFFRAC for the rigid TLP. (The dotted lines correspond to difference frequencies of $\pm\omega_1$, the surge eigenfrequency.)

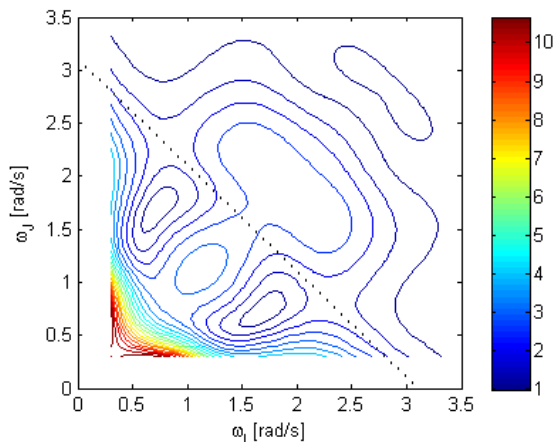


Fig. 4: Nondimensional amplitude of pitch sum-frequency QTF of DIFFRAC for the rigid TLP. (The dotted line corresponds to sum frequencies of ω_5 , the pitch eigenfrequency for the fully rigid TLP.)

Simplifications and reference to other studies

Before going on with further description of the load cases and the presentation of the results, let us state what the main simplifications were for the modeling followed in this study.

- TLP dynamics were heavily simplified by using a spring to model all tendons. The effect of the dynamics of the tendons

was totally ignored in this way. Obviously, no slack tendon event could be modeled. Other studies have included the modeling of the tendons together with the effect of second-order wave loading. Bae and Kim (2013) found that sum-frequency second-order wave loads resulted in an increased standard deviation by 20% of the upwind and downwind tethers in a parked condition. It is noted that the TLP considered by Bae and Kim had a displacement twice that of the DeepCwind TLP, and therefore much larger second-order wave loads could be expected than for the present study.

- The environment consisted of a few sea-states of long-crested waves with zero-deg heading. This wave direction enabled us to focus on the surge, heave and pitch, or first tower fore-aft bending mode and ignore the sway, roll and yaw. In the present study, extreme waves were chosen to track down the effect of second-order wave loads on the motion responses. Bachynski And Moan (2014) looked at more realistic environmental conditions including misaligned wind and waves in the fatigue study of four TLP foundations for wind turbines. Despite the larger displacement of these TLPs (+48% for the smallest TLP), she found that the effect of the second-order wave loads on the fatigue damage was small.
- Although the wave excitation was calculated up to the second order, the wave description was still taken as linear. Responses related to non-linearity in the waves (other than the contribution of the second-order velocity potential in the QTFs) were out of the scope of this study (i.e., the effect of steep or breaking waves are not looked at). Whereas ringing loads were identified as a serious threat for TLP with a pitch natural period of 3-4 s (Bachynski and Moan, 2014), ringing is not investigated in this paper.
- The viscous damping was modeled as a set of linear damping coefficients for each rigid-body mode. Only the coefficient in surge was determined from the results of a surge-decay model test at MARIN. The same coefficients were used for the fully rigid TLP and the TLP with the flexible tower. As the viscous damping coefficients in heave and pitch could not be determined from the decay tests at MARIN with enough accuracy, they were arbitrarily chosen.
- The aerodynamic damping and other turbine operational effects were omitted. These effects were taken into account by Bae and Kim (2013) and shown to mask the response to second-order wave loads for a larger TLP with the same 5-MW turbine on top in operational condition.

Based on the recommendations of recent research work at NREL (Matha, 2009; Roald, Jonkman, Robertson and Chokani, 2013), the main targets of this work were:

- Modeling the TLP in {WAMIT+FAST} with the recently available second-order loads and its comparison with a similar combination of tools {DIFFRAC+aNySIM}.
- The effect of the flexibility of the tower on the simulation results of FAST. Only the lowest structural mode of the tower was considered (first bending mode) because this mode combines with the pitch rigid-body mode of the TLP at a low frequency.

Load Cases

This section describes the load cases (LC) applied to the systems in this comparison study. Other studies that included second-order wave loading on TLP foundations for wind turbines (Bae and Kim, 2013; Bachynski and Moan, 2013) showed that these effects were mostly

noticeable in the most extreme wave conditions with parked turbines. Therefore, load cases with only waves were chosen for this study.

Load cases LC2.2 and LC2.5 of the OC4 benchmark study (Robertson, Jonkman, Masciola, Song, Goupee, Coulling and Luan, 2012) were chosen for the simulations, but applied in this paper to the TLP. In LC2.2, the floater was exposed to a mono-directional JONSWAP wave spectrum with a significant wave height (H_s) of 6 m, a peak period (T_p) of 10 s, and a peak enhancement factor (γ) of 2.87. LC2.5 stands for a 50-year extreme sea-state, made of a JONSWAP mono-directional spectrum with H_s of 15 m, T_p of 19.2 s and γ of 1.05. A first-order cutoff frequency was set at 1.57 rad/s. This value was chosen smaller than the smallest pitch/tower first bending mode as will be seen later (cf Towers section). The cutoff frequency is used to segregate the effects of first-order wave loads and second-order wave loads. Fig. 5 displays the cutoff frequency in a green vertical dashed line. LC2.2 was also generated with no cutoff frequency (“LC2.2 NCOF” in Fig. 5). A broad band wave spectrum was also simulated; this “white noise” wave (LCWN in Fig. 5) was generated in the same direction and without spreading as for LC2.2 and LC2.5, but this time, the wave energy spreads across the entire range of frequencies ([0.3-7.0] rad/s). This load case (completely unreal) was used to determine the motion RAOs for the considered systems. Therefore, only first-order wave loads are applied in this load case. All these wave Power Density Spectra (PSD) are plotted on the same graph in Fig. 5. The following annotation is used for the loading conditions applied during the simulations:

- LC2.2-F1: LC2.2 wave with a cutoff frequency at 1.57 rad/s, first-order wave loads only are applied.
- LC2.2-F1-NCOF: LC2.2 wave without a cutoff frequency, first-order wave loads only.
- LCWN-F1: White-noise with a very high cutoff frequency of 7 rad/s, first-order wave loads only are applied.
- LC2.2-ALL: LC2.2 wave with a cutoff frequency at 1.57 rad/s, all components of first- and second-order loads are applied.
- LC2.5-F1-NCOF: LC2.5 wave without a cutoff frequency, first-order wave loads only.
- LC2.5-ALL: LC2.5 wave with a cutoff frequency at 1.57 rad/s, all components of first- and second-order loads are applied.

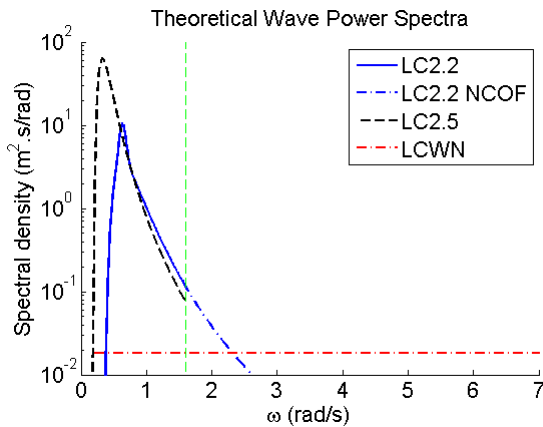


Fig. 5: Wave spectra used in simulations.

Summary of the Comparison Study for the Rigid TLP

The motion responses of the rigid TLP of {DIFFRAC+aNySIM} and {WAMIT+FAST} were compared.

The first-order responses to the waves were checked through the comparison of RAOs for surge, heave, and pitch from the results of aNySIM and FAST for LC2.2-F1. These RAOs were plotted with those of the linear solution of the potential-flow problem (i.e., DIFFRAC and WAMIT), and the match was found to be excellent (Gueydon, Wuillaume, Jonkman, Robertson and Platt, 2015).

In a second step, the second-order wave loads were added to the linear wave loads in aNySIM and FAST. For the rigid TLP, no major differences could be seen between the results of {DIFFRAC+aNySIM} and {WAMIT+FAST} (Fig. 6). As a result, and because aNySIM could not be run for a TLP with flexible tower, the remainder of the results presented in this paper use a mixed solution of DIFFRAC+FAST (the DIFFRAC output was converted to WAMIT format for this solution). For this part of the work, DIFFRAC was preferred to WAMIT for practical reasons as these calculations were carried out by MARIN.

The effects of the second-order loads were very small, and the results of the simulations of LC2.2-ALL and LC2.2-F1 were practically equal (Fig. 7). The difference-frequency second-order loads caused no visible variation of the surge motion. No other noticeable variation was caused by the sum-frequency second-order loads for the rigid TLP due to the very high natural frequencies in heave and pitch (Table 3).

Running these simulations again with the official release of FASTv8.10 did not change these results.

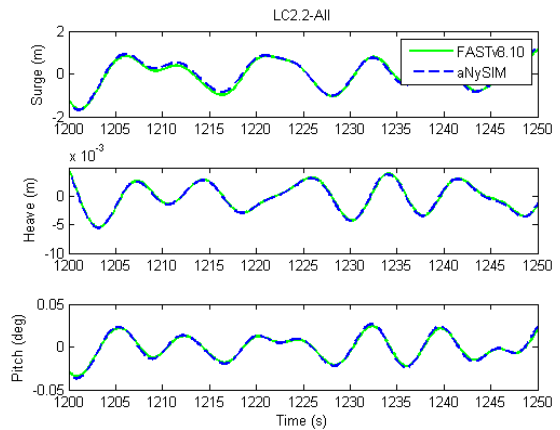


Fig. 6: Comparison of rigid TLP motions {DIFFRAC+aNySIM} and {WAMIT+FAST} for load case LC2.2-ALL.

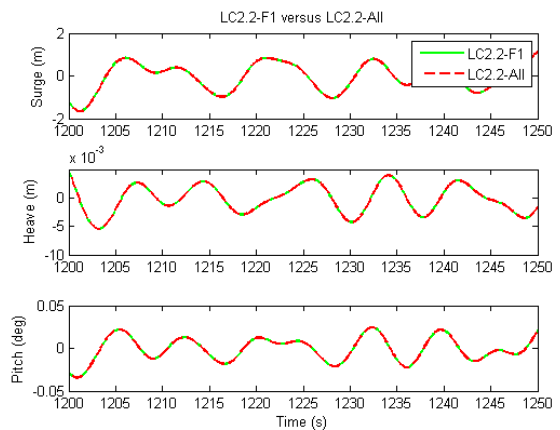


Fig. 7: Effects of second-order loads on motions in comparison to first-order simulations with FAST v8.10 for the rigid TLP.

Numerical Approach for the Flexible TLP

During the MARIN experiments, it was observed that the pitch eigenfrequency was lower than the value in Table 3. This can be explained by the effect of the structural flexibility of the model, especially the tower. Molin, Remy and Facon (2004) and Matha (2009) showed that the flexibility of the tower is the main cause of the decrease of the pitch eigenfrequency as this mode is coupled with the first tower-bending mode. Using FAST, the flexibility of the tower can be accounted for by including six degrees of freedom (DOFs) for the motion of the TLP foundation, plus additional DOFs to represent the deformation modes of the tower (one extra per bending mode). Table 4 gives the eigenmodes calculated by FAST. In this way, the response of the TLP with a flexible tower can be simulated by FAST. Other studies have already looked at the response of TLPs for wind turbines to second-order wave loads, accounting for the elasticity of the tower (Bae and Kim, 2013; Bachynski and Moan, 2013). These works have confirmed that second-order sum-frequency loads have an effect in parked condition. However, these studies were done with a TLP larger than the DeepCwind TLP. As a main addition to previous studies, the present work accounts for the effect of the tower flexibility in the determination of the second-order QTF. Also, the full difference-frequency QTF is applied in the present work whereas previously mentioned studies used the Newman approximation.

Using the correct first-order motion response is important to determine the second-order excitation loads as the second-order term results from the multiplication of two first-order quantities. Thus, the pitch response, which is affected by the elasticity of the tower, cannot be ignored for the calculation of the second-order loads. However, the number of DOFs for a TLP is fixed to six for a single rigid body in DIFFRAC and WAMIT. As a consequence, there is no direct way to include the effect of the tower's flexibility in the hydrodynamic database of the TLP. A workaround for approximating the effect consists of substituting the pitch response of the rigid body by its pitch response with the flexible tower. In other words, the pitch resonance peak of the TLP can be shifted to the new frequency influenced by the tower's first bending mode. Note that in the present case, ω_5 of Table 4 became the new pitch frequency in place of ω_5 of Table 3. In this approach, the total stiffness coefficient in pitch ($C_{55}+K_{55}$) is adjusted so that the resonance peak occurs at the eigenfrequency of the TLP with the flexible tower. Fig. 8 shows how the new equivalent stiffness was determined. The upwards triangle marker corresponds to ($C_{55}+K_{55}$) of the rigid TLP (at 3.1 rad/s), and the downwards triangle marker gives the equivalent value of ($C_{55}+K_{55}$) for the TLP with the flexible tower (at 1.8 rad/s). The new value of the total stiffness in pitch (and roll) was $2.3E10$ N.m/rad for this case.

Acknowledging that only the pitch and roll are affected by the elasticity of the tower, not the other modes, the stiffness values for surge, sway, heave and yaw stay equal to the values used for the rigid TLP. The first-order motion response amplitude operators (RAOs) (Fig. 9) are then obtained with the corrected stiffness in pitch (and roll), and these responses are used in the calculation of the second-order excitation loads. As a result, new QTFs can be calculated (Fig. 10). For the present case, it was observed that the surge difference-frequency QTFs looked almost identical whether the pitch response of the rigid or the flexible body was used. The pitch sum-frequency QTF looked a bit different. The amplitudes of its peaks were slightly higher, and their locations were different. However, these differences can be considered as minor. More importantly, the lines corresponding to the sum-frequency equal to the pitch eigenfrequencies with or without the tower flexibility crossed the QTFs in very distinct sections. These new QTFs can finally be used for the simulations of the second-order wave loads

on the TLP with a flexible tower, and its motion can be compared to the motions of the fully rigid TLP. This whole exercise aims to understand what the impact is of second-order wave loads on the motions of the TLP with a flexible tower.

Table 4. Eigenfrequencies of the moored TLP with the turbine on top, modeled with a flexible tower.

Eigenfrequency	Symbol	Units	Values
Translation along x axis (Surge)	ω_1	rad/s	0.15
Translation along z axis (Heave)	ω_3	rad/s	6.3
Pitch/tower first bending mode	ω_5	rad/s	1.8
Pitch/tower second bending mode	ω_7	rad/s	>7.0

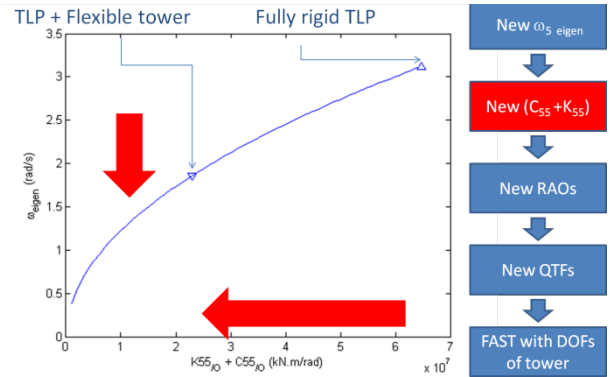


Fig. 8: Eigenfrequency in pitch as a function of the pitch stiffness.

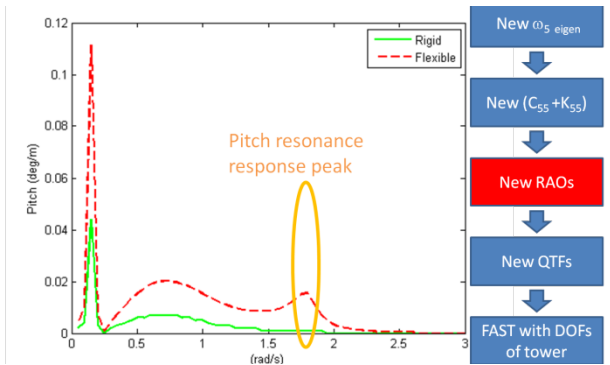


Fig. 9: Pitch response first-order RAOs with both a rigid and flexible tower used for the second-order calculation.

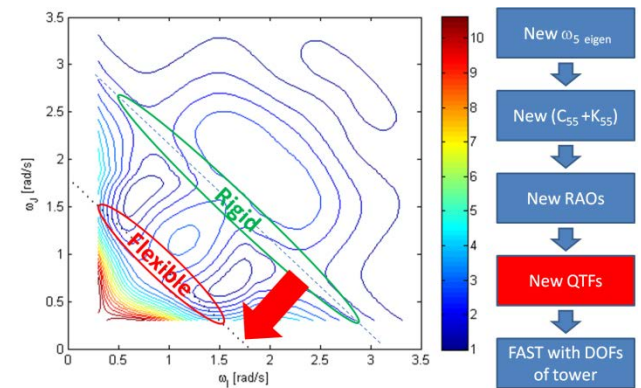


Fig. 10: Shift of ω_5 for the TLP with the flexible tower in the sum-frequency QTF in pitch.

The approach described above was taken for two towers of different stiffness to investigate the combined effect of second-order wave loads and the tower's flexibility on the motions of the TLP. Using two different towers makes it possible to explore the effect of having a pitch resonance frequency in ranges where the level of second-order wave loads is different.

Towers

Shortening the tower's length (and hub height) is a straightforward way to stiffen the tower and consequently increase the pitch eigenfrequency of the system. For the purpose of studying the response of the TLP to second-order wave loads, two different tower lengths were used:

- The original tower length: 87.6 m.
- A tower shortened by 10 m: 77.6 m.

Except from the length, the towers have the same properties (diameter, structural properties). The rest of the turbine, the floater and the tendons were unchanged. The TLP for these two towers was simulated with the towers considered rigid and flexible, resulting in the simulations of four systems:

- Rigid O: TLP + rigid (R) tower of original (O) length
- Flexible O: TLP + flexible (F) tower of original(O) length
- Rigid S: TLP + rigid (R) tower with shortened (S) length
- Flexible S: TLP + flexible (F) tower of shortened (S) length

Table 5. Pitch eigenfrequencies ω_5 of the moored TLP with the different towers.

Tower model	Units	ω_5
Rigid O	rad/s	3.1
Flexible O	rad/s	1.8
Rigid S	rad/s	3.7
Flexible S	rad/s	2.2

New Results for the TLP with Flexible Tower

The QTFs, which were calculated for the TLP with flexible towers, differed only by a few percent from the QTFs for the rigid TLP (see results for tower O in Fig. 11). The motion responses of the TLP with a flexible tower were compared to those of a fully rigid system. The FAST results are shown in Fig. 12. It is observed that the tower's flexibility affects only the pitch rotation: the surge and heave motions of the TLP with a flexible tower are unchanged compared to those of the fully rigid TLP. The pitch rotation is slightly increased, and it is subjected to little more frequent variations with the flexible tower than with the rigid tower. On the other hand, this increase in the pitch response is far less important than what was observed earlier with a prototype version of FAST v8 (Fig. 13). The comparison between the simulations with a flexible tower and a rigid tower was also done for the other load cases. The most instructive plots are included in this paper:

- Fig. 14 for LC2.2-F1 comparing Rigid O and Flexible O.
- Fig. 15 comparing results of LC2.2-F1 and LC2.2-F1-NCOF for Rigid O and Flexible O.
- Fig. 16 comparing results of the original tower with those of the shorter tower for LC2.5-All.

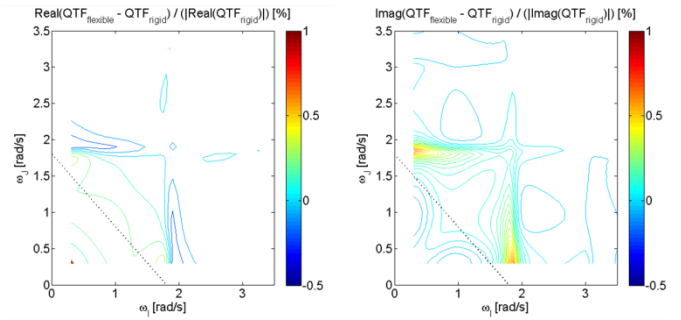


Fig. 11: Difference between Flexible O and Rigid O tower in real and imaginary part of the pitch sum-frequency QTFs.

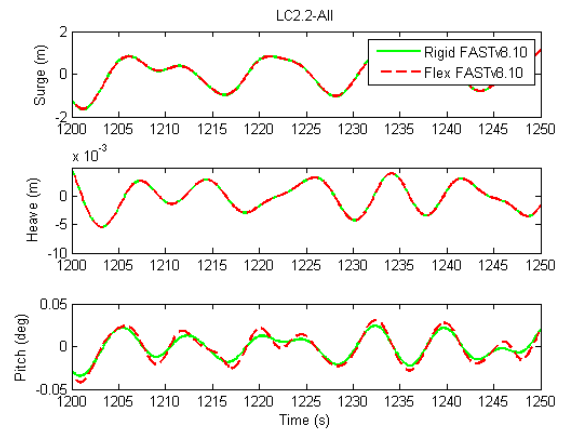


Fig. 12: Effects of tower's flexibility on TLP motions for LC2.2-All (Rigid O versus Flexible O).

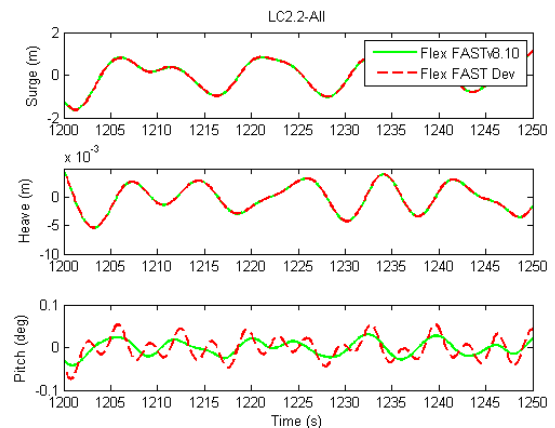


Fig. 13 Difference between prototype version (FAST Dev) and official release of FAST v8.10 for LC2.2-All for Flexible O.

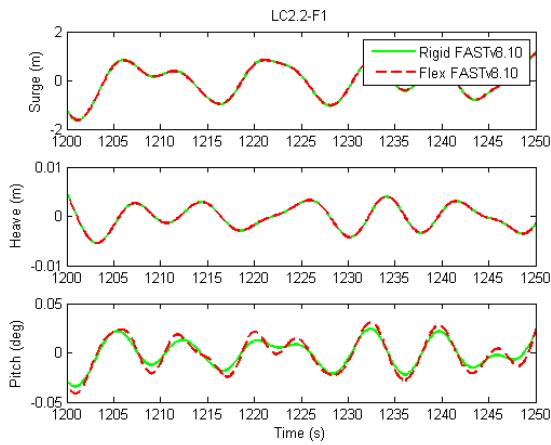


Fig. 14: Effects of tower's flexibility on TLP motions for LC2.2-F1 (Rigid O versus Flexible O)

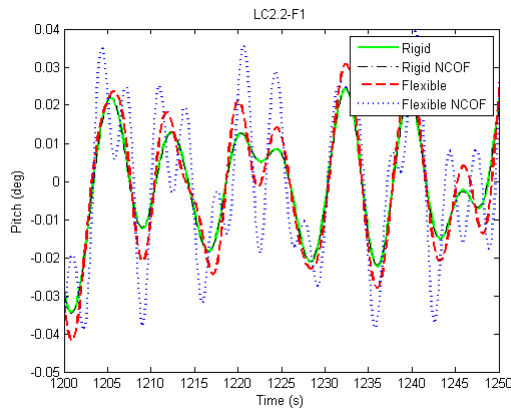


Fig. 15: Effect of cutoff frequency on TLP's pitch for LC2.2-F1.

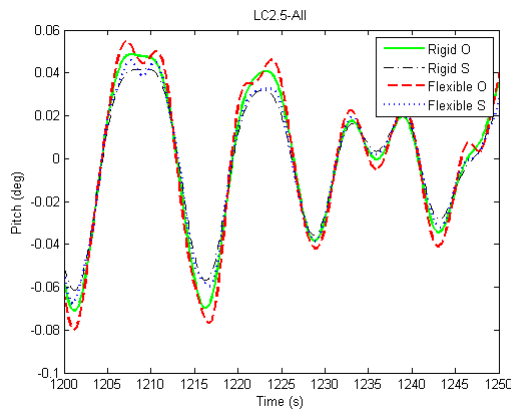


Fig. 16: Effects of tower's flexibility on pitch rotation for LC2.5-All.

From the observation of Figs. 12 and 14, we can already deduce that the tower's flexibility is having a large impact on the first-order wave response. Fig. 15 demonstrates that the cutoff frequency has a big impact on the increase of the pitch variation for the flexible tower whereas it has no impact for the rigid tower. Also, using towers of different flexibilities changes the pitch results (Fig. 16). As would be expected for a linear response, the system with the stiffer pitch/first tower-bending mode (Flexible S) restrains the pitch rotation more than the less stiff system (Flexible O).

DISCUSSION

Rigid TLP

All results of this comparison study showed that the motion response of the TLP is mainly linear. This finding was expected as the mooring system was modeled with a spring matrix, the second-order excitation is much smaller than the first-order wave loads, and the natural frequencies are outside the wave-excitation range. In surge, the second-order difference-frequency excitation occurs in a frequency range that includes the eigenfrequency, but these loads are so small that they have no visible impact on the surge motion. These results are identical to those reported earlier with the prototype version of FAST v8 (Gueydon, Wuillaume, Jonkman, Robertson and Platt, 2015).

TLP with Flexible Tower

Fig. 17 contains the PSDs of the first- and second-order wave load contributions for the TLP with the original flexible tower for LC2.2. The black dashed curve corresponds to the case when no cutoff frequency is used in the calculation of first-order wave loads. Fig. 18 shows the same quantities for the short flexible tower and for LC2.5. The excitation PSDs are plotted together with the eigenfrequencies for the surge mode, the heave mode and the pitch/first-tower bending mode. As explained before, only the pitch eigenfrequency changes when the tower is modeled as a flexible body. The eigenfrequency in pitch of the system with the original tower is located just between the linear wave excitation range and the sum-frequency second-order wave load range, whereas it lies in the middle of the pitch sum-frequency excitation range (2–3 rad/s) for the short tower. In this frequency range, the second-order sum-frequency loads are larger than the first-order wave loads for the TLP with the short tower. Therefore, the system with the short tower is better to investigate possible effects of the second-order wave loads on pitch than the TLP with the original tower. However, it should be noted that these loads remain much smaller than first-order wave loads. Moreover, the pitch eigenfrequency of the original flexible tower is low enough to be excited by first-order wave moment in pitch when no cutoff frequency is used.

The shift towards a lower frequency when considering tower flexibility may in principle increase the exposure to first- and second-order wave loads. PSDs of the pitch motion resulting from FAST simulations with and without the flexibility of the tower are compared in Fig. 19. Under linear wave excitation and second-order wave loading, the PSD of the flexible TLP does not differ much from the PSD of the rigid system. Minor differences can be found at the wave excitation peak (0.7 rad/s) and just below 1.8 rad/s, the pitch eigenfrequency of Flexible O. Despite what was observed earlier with the prototype version of FAST v8 for LC2.2 and the original tower (Gueydon, Wuillaume, Jonkman, Robertson and Platt, 2015), no significant increase in the response in pitch are caused by the second-order wave loads with the official release of FAST v8.10 whether the flexibility of the tower is accounted for (Fig. 19) or not. The change in the pitch response of Flexible O between these two versions of FAST is particularly visible at the eigenfrequency (Fig. 20). In FAST v8.10, the increase of the pitch response for the TLP with the flexible tower is due to the linear wave loads as Figs. 21 and 22 confirm. Indeed, the zoom around the wave response peak shows an increase of the response that is directly related to the reduction of the stiffness in pitch. This increase acts over a large part of the wave spectrum range. Next to this increase, the pitch response is also locally amplified around the pitch eigenfrequency, which has shifted from a high value for the rigid tower (3.1 rad/s, see the green dashed vertical line in Fig. 21) to a lower value for the flexible tower (1.8 rad/s, see the red vertical dashed line in Fig. 21). This last cause of amplification is actually a resonance phenomenon as it occurs solely because the frequency of excitation matches the natural period of the system. This resonant peak becomes dominant when no

cutoff frequency is used for the wave spectrum (see the curve “NCOF Flexible” in Fig. 21). As seen in the previous paragraph, the TLP with the short tower is more susceptible to reacting to second-order wave excitation because the eigenfrequency is shifted to the middle of the range where these loads are at a maximum. The pitch PSD for all towers is plotted on the same graphic (Fig. 22) to observe how the two causes of pitch response increase compare to each other for the most extreme wave (LC2.5). The mechanism is identical for the short tower; two effects are superposed:

- Linear wave response
- Resonance response.

When the tower is considered flexible, the stiffness in pitch is decreased and the eigenfrequency shifts to a lower value (vertical blue dotted line for the short tower in Fig. 22). This apparent stiffness reduction provokes an increase of the wave response peak relative to the response of the TLP with the rigid tower. This increase is moderate, but it is spread over a large range of frequencies around the wave response peak. Note that this part of the response varies linearly with the wave height. In parallel, the response to the wave loads (first and second order) is amplified around the new pitch eigenfrequency in a local resonance peak. For the tower S, this value is higher than for the tower O. As a consequence, the amplification acts this time exclusively on the response to sum-frequency second-order wave loads, which are quadratic to the wave height. As the peak around 2.2 rad/s (blue dotted line) indicates, the second-order wave loads are largely dominant around the eigenfrequency of the flexible tower S. Nevertheless, the level of the response peak to the second-order wave loads is still small and does not exceed the response to the linear wave loads on the tail of the wave spectrum (between 1-1.5 rad/s). This is a confirmation that second-order wave loads are not a concern for the pitch response of this TLP even with a stiffer tower in the most extreme waves. Only the linear wave loads can provoke a significant increase of the pitch response of the TLP with flexible tower when the resonance amplification occurs as a result of the apparent shift of eigenfrequency in pitch to a lower value. This is precisely what happened in LC2.2 for the TLP with the flexible tower O. The conjunction of second-order wave loads and tower flexibility does have an impact on the tower structural loads (tower base pitch moment in Fig. 23) but this impact is small for LC2.5. Nevertheless, the impact on the fatigue damage, which is not looked at here, should also be considered before a decision to neglect the sum-frequency second-order wave loads could be taken (Bachynski and Moan, 2014).

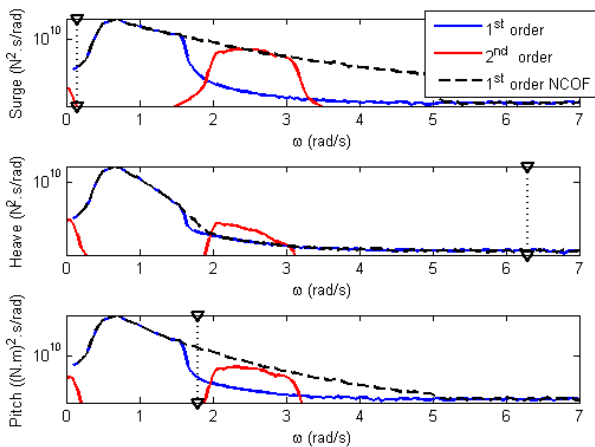


Fig. 17: PSDs of all first- and second-order contributions to the wave loads for Flexible O in LC2.2-All and in LC2.2-F1-NCOF. Vertical markers indicate the eigenfrequencies.

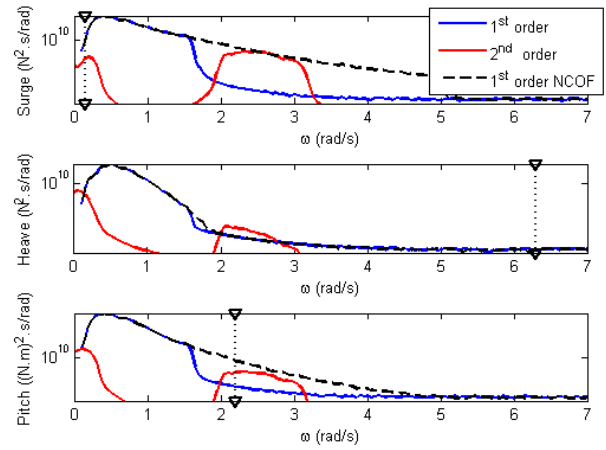


Fig. 18: PSDs of all first- and second-order contributions to the wave loads for Flexible S in LC2.5-All and in LC2.5-F1-NCOF. Vertical markers indicate the eigenfrequencies.

Coming back to the results obtained with the prototype version (Gueydon, Wuillaume, Jonkman, Robertson and Platt, 2015), it is demonstrated (Fig. 20) that the sum-frequency second-order wave loads were wrong. It can also be said that the problem in the prototype version, still in development at the time it was used, was strictly related to the second-order wave loads. An exaggeration of these second-order wave loads led to an amplified pitch response in the previous attempt to analyze the TLP with the flexible tower (Gueydon, Wuillaume, Jonkman, Robertson and Platt, 2015). This problem was solved before the first official release of FAST that included the second-order wave loads (FAST v8.10). Therefore, the results of the present paper on the TLP with the flexible tower replace the results of the paper of 2015 (Gueydon, Wuillaume, Jonkman, Robertson and Platt, 2015).

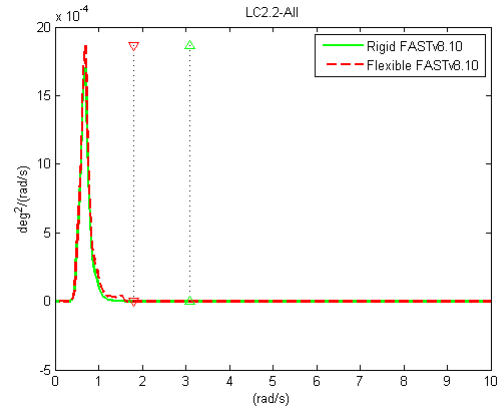


Fig. 19: Effect of tower’s flexibility on the pitch responses (PSD) for simulations with first- and second-order wave loads (LC2.2-ALL) for the tower O.

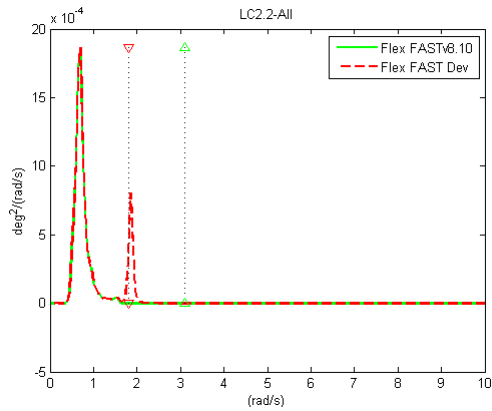


Fig. 20: Difference in the pitch responses (PSD) for simulations with the prototype of FAST and the official release v8.10 (LC2.2-ALL) for Flexible O.

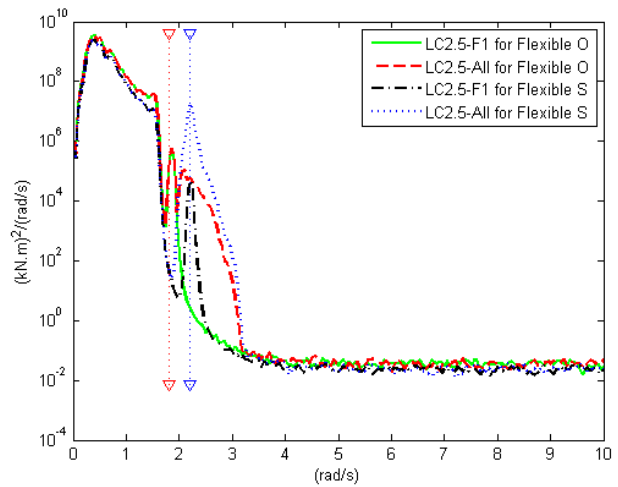


Fig. 23: Effect of second order wave loads on tower base moment in pitch for the flexible towers (O and S).

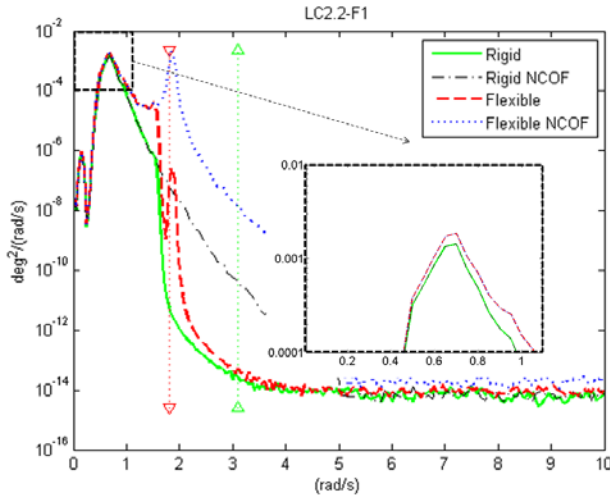


Fig. 21: Effect of cutoff frequency on TLP's pitch for LC2.2-F1 with the tower O.

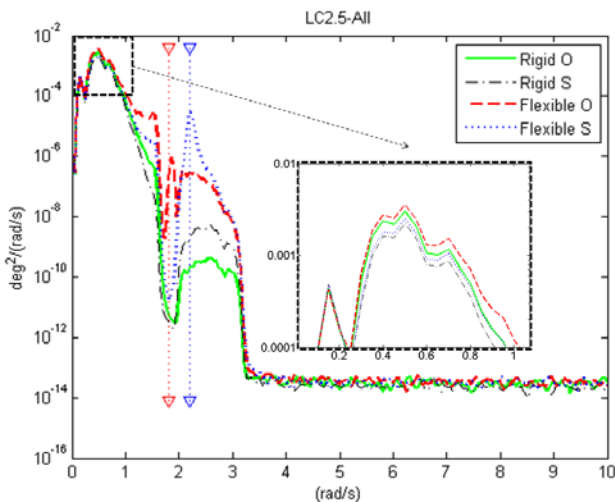


Fig. 22: Effects of tower's flexibility on pitch motions for LC2.5-All for both towers (O and S).

CONCLUSIONS

Two numerical packages, {DIFFRAC+aNySIM} and {WAMIT+FAST}, were compared using a TLP platform supporting a wind turbine. This comparison was done with the assumption that the TLP is a fully rigid body. The results of both packages in long-crested head waves were very close to each other. The TLP, seen as a fully rigid body, appeared to be little sensitive to second-order wave loads. Indeed, only a small effect on the surge motion could be noticed.

A work-around was proposed and applied in this study to include the flexibility of the tower in the calculation of the second-order QTFs. In this approach, the stiffness in pitch was adjusted during the second-order potential-flow calculation to better reproduce the pitch response of the TLP with a flexible tower. The adjusted QTFs were found to be very similar to the original QTFs. The comparison of the motion results of the TLP with the flexible tower against those of the fully rigid TLP showed that only the pitch motion was affected by the tower's flexibility. This finding can also be extended to the roll motion when wave headings other than head-waves or stern waves are considered. The increase of the pitch response for a narrow wave spectrum was very small, but it got bigger for a broader spectrum (when no cutoff frequency was used). This augmentation of the pitch response is made of two components:

- The raise of the response to wave (linear) excitation in conjunction with the pitch stiffness decrease. This augmentation is moderate, but it is spread across a large range of frequencies.
- The possible exposure to a resonance phenomenon while the pitch eigenfrequency is shifted to a lower frequency. This amplification can be big, but it is local around the eigenfrequency.

For the TLP studied, the resonant amplification of first-order wave loads occurred when no cutoff frequency was used. This had a great impact on the pitch motion whereas the resonance of second-order loads could be disregarded as the corresponding pitch moments were too small. Therefore, the influence of the first-order cutoff frequency is large. For the stiffer tower (Flexible S), the cutoff frequency actually determines whether the pitch resonance is from first- or second-order wave excitation.

In conclusion, the most important effect caused by the tower's flexibility is the apparent shift of the pitch eigenfrequency and the associated apparent decrease of the overall stiffness in pitch of the TLP.

In this work, the combined effects of second-order wave loads and the flexibility of the tower were studied assuming a linear stiffness matrix for the tendons. Also, this study gave most of attention to the motions of the TLP. In potential future work, the impact of the TLP set-down from a non-linear treatment of the tendons could be considered and the structural loads could be examined. Other studies have looked at the effects of these loads on larger TLPs including a dynamic model of the tendons and for more realistic environmental conditions (Bae and Kim, 2013; Bachynski and Moan, 2014). They found that the impact of sum-frequency second-order loads was small for operational conditions but more important for parked conditions. The tendon tension was found to be more sensitive to second-order loads than the tower bending moment (Bachynski and Moan, 2014).

ACKNOWLEDGEMENTS

The authors are obliged to the DeepCwind consortium led by the University of Maine for the experience gained from the model-test campaign. The work of Pierre-Yves Wuillaume on the comparison of {DIFFRAC+aNySIM} and {WAMIT+FAST} during his internships at MARIN and NREL is acknowledged, as it was the foundation on which this study was built. The active participations of other colleagues at NREL and MARIN in the first part of this work are also acknowledged.

REFERENCES

Bae, YH and Kim, MH (2013). "Turbine-floater-tether coupled dynamic analysis including second-order sum-frequency wave loads for a TLP-type FOWT (floating offshore wind turbine)," *32nd International Conference on Ocean, Offshore and Arctic Engineering*, Nantes.

Bachynski, EE and Moan, T (2014). "Second order wave force effects on tension leg platform wind turbines in misaligned wind and waves," *33rd International Conference on Ocean, Offshore and Arctic Engineering*, San Francisco.

Bachynski, EE and Moan, T (2014). "Ringing Loads on Tension Leg Platform Wind Turbines", *Ocean Engineering*, 84, 237-248.

Bunnik, T (2012). *DIFFRAC version 2.4 User Guide*, MARIN, Wageningen.

Goupee, AJ, Koo, BJ, Lambrakos, KF and Kimball, RW (2012). "Model Tests for Three Floating Wind Turbine Concepts," *Proc. 2012*

Offshore Technology Conference, Houston.

Gueydon, S, Duarte, T and Jonkman, J (2014). "Comparison of Second-Order Loads on a Semisubmersible Floating Wind Turbine," *33rd International Conference on Ocean, Offshore and Arctic Engineering (OMAE)*, San Francisco.

Gueydon, S, Wuillaume, PY, Jonkman, J, Robertson A and Platt A (2015). "Comparison of Second-Order Loads on a Tension Leg Platform for Wind Turbines," 2015-TPC-0400, *Proc. of the ISOPE Int'l Society of Offshore and Polar Engineers*, Kona.

Jonkman, J and Buhl, Jr., ML (2005). *FAST User's Guide: Updated August 2005*, Tech. Rep. NREL/TP-500-38230, National Renewable Energy Laboratory.

Lee, CH and Newman, JN (2013). *WAMIT – User manual version 7.0*, WAMIT Inc., Chestnut Hill, Massachusetts.

Maritime Research Institute Netherlands (2009). *aNySIM User Guide*, MARIN, Wageningen <https://wiki.marin.nl/index.php/ANYwiki>

Matha, D (2009). *Model Development and Loads Analysis of an Offshore Wind Turbine on a Tension Leg Platform, with Comparison to Other Floating wind Turbine Concepts*, Master's thesis, University of Colorado-Boulder.

Molin, B, Remy, F and Facon, G (2004). "Etude experimental du comportement hydro-aero-elastique d'une eolienne offshore sur ancrage tendus," *Ocean Energy Conference*, Brest, France.

Prowell, I, Robertson, A, Jonkman, J, Stewart, G and Goupee, A (2013). "Numerical Prediction of Experimentally Observed Scale-Model Behavior of an Offshore Wind Turbine Supported by a Tension-Leg Platform," *Proc. 2013 Offshore Technology Conference*, Houston.

Roald, L, Jonkman, J, Robertson, A and Chokani, N (2013). "The Effect of Second-order Hydrodynamics on Floating Offshore Wind Turbine," NREL, Golden, Colorado.

Robertson, A, Jonkman, J, Masciola, M, Song, H, Goupee, A, Coulling, A and Luan, C (2012). *Definition of Semisubmersible Floating System for Phase II of OC4*, Technical Report NREL/TLP-5000-60601.

Robertson, A, Fabien, V and OC4 Participants (2014). "Offshore Code Comparison Collaboration Continuation Within IEA Wind Task 30: Phase II Results Regarding a Floating Semisubmersible Wind System," *33rd International Conference on Ocean, Offshore and Arctic Engineering (OMAE)*, San Francisco.

Wuillaume, PY (2014). *Comparison of DIFFRAC, WAMIT, aNySIM and FAST*, Internship's report, Ecole Centrale de Nantes.